radii. The separation of the iodine atoms of molecule II and molecule I (x, y, $z-1$) is 4·22 Å which means that they are in van der Waals contact, but there is no close approach to the iodine atoms comparable with that reported for 5-iodo-2′-iododeoxyuridine (Camerman & Trotter, 1965).

The authors thank Professor J. Iball for guidance in the use of the four-circle diffractometer and Dr P. Tollin, Dr D. W. Young and Mr A. R. I. Munns for discussion. We also thank Mr J. Low for assistance with the data collection and Miss Pauline Hendry for computational assistance. A Science Research Council grant for the purchase and maintenance of the Hilger and Watts linear diffractometer, and financial aupport by the Medical Research Council are gratefully acknowledged.

References

ARNOTT, S., DOVER, S. D. & WONACOTT, A. J. (1969). *Acta Cryst.* B**25**, 2192.
ARNOTT, S. & HUKINS, D. W. L. (1969). *Nature, Lond.* In the press.
CAMERMAN, N. & TROTTER, J. (1965). *Acta Cryst.* **18**, 203.
COULTER, C. L. (1968). *Science,* **159**, 888.
DONOHUE, J. (1967). In *Structural Chemistry and Molecular Biology.* Edited by A. RICH and N. DAVIDSON. San Francisco: Freeman.
DONOHUE, J. & TRUEBLOOD, K. N. (1960). *J. Mol. Biol.* **2**, 363.
HARRIS, D. R. & MACINTYRE, W. M. (1964). *Biophysical J.* **4**, 203.
HASCHEMEYER, A. E. V. & RICH, A. (1967). *J. Mol. Biol.* **27**, 369.
IBALL, J., MORGAN, C. H. & WILSON, H. R. (1968). *Proc. Roy. Soc. A*, **302**, 225.
International Tables for X-ray Crystallography (1962). Vol. III. Birmingham: Kynoch Press.
MUNNS, A. R. I., TOLLIN, P., WILSON, H. R. & YOUNG, D. W. (1970). *Acta Cryst.* B**26**, 1114.
NAGASHIMA, N. & IITAKA, Y. (1968). *Acta Cryst.* B**24**, 1136.
NICE, E. G. & RORKE, D. (1969). *Int. J. Radiat. Biol.* **15**, 197.
PIMENTEL, G. C. & MCCLELLAN, A. L. (1960). *The Hydrogen Bond.* San Francisco: Freeman.
RAHMAN, A. & WILSON, H. R. (1970). *Nature, Lond.* **225**, 64.
SAENGER,W. & SCHEIT, K. H. (1968). *Angew. Chem.* **81**, 121.
SINGH, C. (1965). *Acta Cryst.* **19**, 861.
SUNDARALINGAM, M. (1965). *J. Amer. Chem. Soc.* **87**, 599.
SUNDARALINGAM, M. & JENSEN, L. H. (1965). *J. Mol. Biol.* **13**, 930.
SHEFTER, E. & TRUEBLOOD, K. N. (1965). *Acta Cryst.* **18**, 1067.
THEWALT, U. T., BUGG, C. E. & MARSH, R. E. (1970). *Acta Cryst.* B**26**, 1089.
WATENPAUGH, K., DOW, J., JENSEN, L. H. & FURBERG, S. (1968). *Science,* **159**, 206.
YOUNG, D. W., TOLLIN, P. & WILSON, H. R. (1969). *Acta Cryst.* B**25**, 1423.

Acta Cryst. (1970). B**26**, 1775

The Crystal Structure and Anisotropic Thermal Expansion of β-Uranyl Dihydroxide, $UO_2(OH)_2$

BY M. J. BANNISTER AND J. C. TAYLOR

Australian Atomic Energy Commission, Research Establishment, Lucas Heights, N.S.W., Australia

(*Received* 7 *August* 1969)

Single-crystal and powder X-ray diffraction techniques were used to determine improved positional, thermal vibration and lattice parameters for the orthorhombic β-$UO_2(OH)_2$. Values obtained for lattice parameters at 21 °C are: $a=5{\cdot}6438\pm0{\cdot}0001$, $b=6{\cdot}2867\pm0{\cdot}0001$, $c=9{\cdot}9372\pm0{\cdot}0002$ Å. Thermal expansion of this material was studied by elevated temperature X-ray diffraction and hot-stage optical microscopy. Thermal expansion up to 260 °C was strongly anisotropic, with large contractions in a, large expansions in b, and a smaller cyclic change in c. Expansion at higher temperatures was almost isotropic. Using the structural and vibrational data, the anisotropic thermal expansion is interpreted in terms of a thermally induced rotation of the oxygen octahedra surrounding all uranium atoms.

Introduction

Single crystals of β-$UO_2(OH)_2$ change in shape during heating to dehydration temperatures. This distortion can be explained if each lattice parameter is measured as a function of temperature. However, interpretation of the thermal expansion results using the crystal structure data of Roof, Cromer & Larson (1964) (hereafter referred to as RCL) is not possible owing to the large standard deviations in the RCL positional and thermal vibration parameters. The structure was therefore redetermined, giving positional and thermal vibration par-

ameters which are both more accurate than, and significantly different from, those of RCL. These improved parameters enable the anisotropic thermal expansion to be explained.

Material

Crystals of the α and β forms of $UO_2(OH)_2$ were produced by heating uranyl nitrate solution with nitric acid and hydrogen in an autoclave at 290 °C and 10·6 MN.m^{-2} and were separated by hand under a stereomicroscope. The β crystals were truncated dipyramids similar in shape to those described by Harris & Taylor (1962). Each was bounded by eight {111} and two {001} faces. The crystal used for structure determination measured 90 by 78 μm between ⟨110⟩ edges and 30 μm between the {001} faces. Those used for hot-stage optical microscopy were generally about twice that size.

Table 1. *Observed and calculated structure factors in* β-$UO_2(OH)_2$

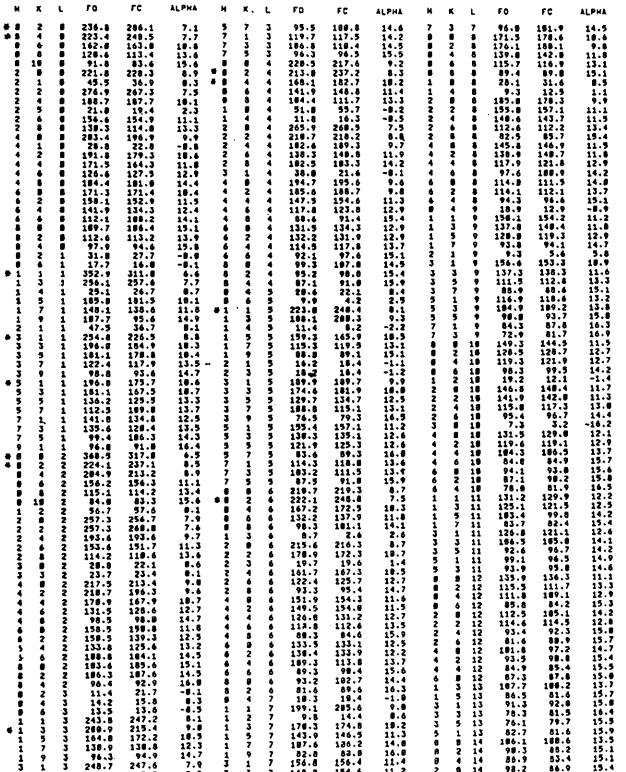

Samples for lattice parameter determination consisted of a few hundred crystals, generally less than 100 μm in maximum dimension, sealed inside 0·5 mm diameter thin-walled silica capillaries.

Crystal structure

Single-crystal X-ray diffraction data were collected, using zirconium-filtered Mo $K\alpha$ radiation, on a General Electric XRD-5 set fitted with a single-crystal orienter and scintillation counter with discriminator. The crystal was mounted about the c axis. 238 strong reflexions of the type h,k,l all even or all odd, and 32 weak reflexions with mixed indices (oxygen scattering only) were measured to $2\theta = 70°$, and all strong reflexions to $2\theta = 50°$ were measured in two octants of reciprocal space. The space group *Pbca* (RCL, 1964) was confirmed. The intensities were corrected for absorption ($\mu = 560$ cm^{-1}) and reduced to $F_o(hkl)$ values using the program *CDRABS* (A.A.E.C. neutron diffraction program library).

Difference syntheses confirmed the RCL structure. The Busing, Martin & Levy (1962*a*) crystallographic least-squares program was modified to include the anomalous dispersion terms $\Delta f' = -9e$ and $\Delta f'' = 9e$ for the uranium atom (Cromer, 1965). Scattering curves used were the self-consistent field curve with exchange for the neutral oxygen atom, and the Thomas–Fermi–

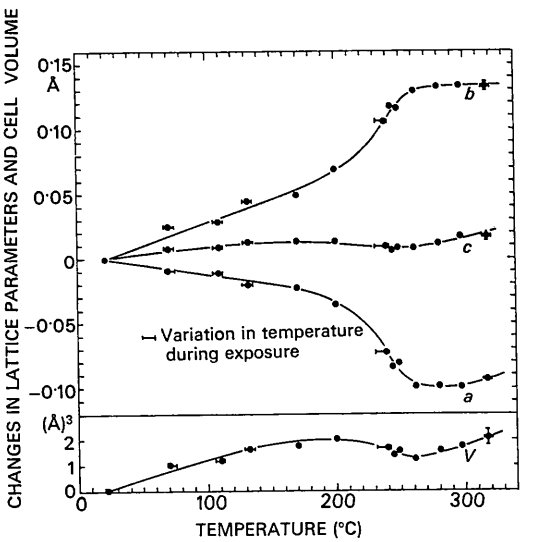

Fig. 1. Changes in lattice dimensions of β-$UO_2(OH)_2$ as functions of temperature.

Table 2. *Positional parameters in* β-$UO_2(OH)_2$ *as found in the present work, compared with the values of Roof, Cromer & Larson* (1964)

	Present work			Roof, Cromer & Larson (1964)		
	x	y	z	x	y	z
U	0	0	0	0	0	0
O(1)	0·154 (3)	0·464 (3)	0·342 (2)	0·137 (9)	0·467 (19)	0·335 (5)
O(2)	0·196 (3)	0·288 (3)	0·082 (2)	0·185 (9)	0·279 (9)	0·093 (5)

Dirac curve for neutral uranium (*International Tables for X-ray Crystallography*, 1962). Isotropic, followed by anisotropic, least-squares refinement with unit weights led to the following overall discrepancy indices:

$$R_1=[\sum(F_o-F_c)^2]^{1/2}/(\sum F_o^2)^{1/2}=0{\cdot}045$$

and

$$R_2=\sum|F_o-F_c|/\sum|F_o|=0{\cdot}041\ .$$

The final list of observed and calculated structure factors is given in Table 1.

A comparison of the F_o and F_c values for the low-angle reflexions shows that errors in the absorption corrections and, probably, extinction, occur in the low-angle data. The reflexions influenced the most by these two effects are marked with asterisks in Table 1 and were not included in the least-squares refinement but were included in the calculation of R_1 and R_2. The fact that F_o exceeds F_c, despite extinction, for the reflexions 002, 111, 311 and 511 (Table 1) suggests that absorption correction errors are at least as large as extinction effects. For this reason, together with the further possibility that extinction may be anisotropic because of the pronounced tendency towards {001} cleavage, it was considered not worth while to apply extinction corrections.

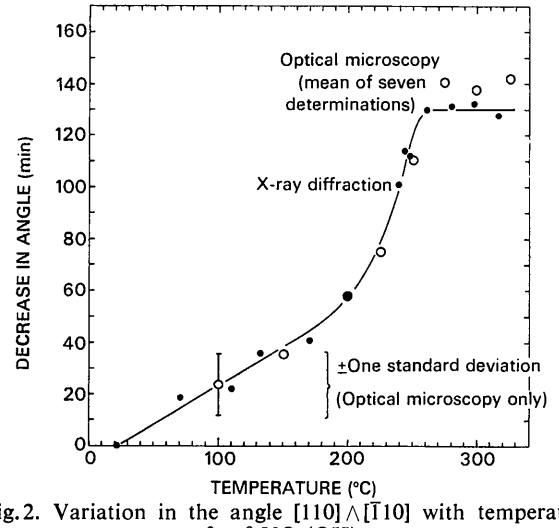

Fig. 2. Variation in the angle [110]∧[$\bar{1}$10] with temperature for β-$UO_2(OH)_2$.

The positional and thermal parameters obtained, together with those of RCL, are listed in Tables 2 and 3. There are slight differences in the oxygen atom positions, and greater differences in the thermal parameters. More importantly, the standard deviations of all parameters are much lower in the present work. All thermal parameters are positive-definite and thus physically reasonable. The improved accuracy is presumed to be largely due to better absorption corrections.

Bond lengths and angles calculated with the program *ORFFE* (Busing, Martin & Levy, 1962*b*) are listed in Table 4 and thermal vibration data, also calculated with *ORFFE*, in Tables 5 and 6. This information is used in a later section to assist interpretation of the thermal expansion results.

Table 4. *Bond lengths and angles in* β-$UO_2(OH)_2$

The letters (*a*), (*b*), (*c*) ... define the operations applied to the coordinates in Table 2. These operations are:

(*a*)	$1+x$	$\frac{1}{2}+y$	$\frac{1}{2}+z$
(*b*)	$1+x$	y	z
(*c*)	$1+x$	$\frac{1}{2}-y$	$\frac{1}{2}+z$
(*d*)	$1{\cdot}5-x$	$\frac{1}{2}-y$	$\frac{1}{2}+z$
(*e*)	$\frac{1}{2}+x$	y	$\frac{1}{2}-z$
(*f*)	$1-x$	$\frac{1}{2}+y$	$\frac{1}{2}-z$
(*g*)	$\frac{1}{2}-x$	$\frac{1}{2}+y$	z
(*h*)	x	y	z

In octahedron

U(*a*)——O(1) (*b*)	1·81 (2) Å
U(*a*)——O(2) (*c*)	2·27 (2)
U(*a*)——O(2) (*d*)	2·32 (2)
O(2) (*c*)–O(2) (*d*)	3·20 (1)
O(2) (*d*)–O(2) (*f*)	3·30 (2)
O(1) (*b*)–O(2) (*c*)	2·88 (3)
O(1) (*b*)–O(2) (*d*)	2·98 (3)
O(1) (*b*)–O(2) (*e*)	2·91 (3)
O(1) (*b*)–O(2) (*f*)	2·93 (3)
O(1) (*b*)–U(*a*)–O(2) (*c*)	88·8 (0·8)°
O(1) (*b*)–U(*a*)–O(2) (*d*)	91·3 (0·8)
O(1) (*b*)–U(*a*)–O(2) (*e*)	88·7 (0·8)
O(1) (*b*)–U(*a*)–O(2) (*f*)	91·2 (0·8)
O(2) (*c*)–U(*a*)–O(2) (*d*)	88·4 (0·4)
O(2) (*d*)–U(*a*)–O(2) (*f*)	91·6 (0·4)

Interlayer contacts

O(1) (*h*)–O(1) (*e*)	3·36 (2) Å
O(1) (*h*)–O(2) (*h*)	2·82 (3)
O(1) (*h*)–O(2) (*g*)	3·40 (3)

Table 3. *Thermal parameters in* β-$UO_2(OH)_2$ *as found in the present work, compared with the values of Roof, Cromer & Larson* (1964)

Temperature factor = $\exp[-(\beta_{11}h^2+2\beta_{12}hk\ldots)]$.

		β_{11}	β_{22}	β_{33}	β_{12}	β_{13}	β_{23}
U	present work	0·0041 (2)	0·0047 (2)	0·0022 (1)	0·0012 (12)	−0·0005 (4)	0·0001 (3)
U	RCL*	0·0041 (9)	0·0116 (9)	0·0047 (4)	0·0020 (28)	0·0019 (15)	0·0033 (7)
O(1)	present work	0·0089 (45)	0·0142 (69)	0·0042 (15)	−0·0009 (44)	0·0022 (23)	−0·0021 (23)
O(1)	RCL	0·0218 (198)	0·1259 (514)	0·0025 (41)	0·0482 (366)	−0·0016 (87)	−0·0097 (157)
O(2)	present work	0·0108 (50)	0·0109 (45)	0·0026 (12)	−0·0057 (39)	0·0018 (22)	0·0002 (22)
O(2)	RCL	0·0288 (206)	0·0197 (157)	0·0043 (40)	0·0160 (181)	−0·0030 (92)	0·0032 (76)

* In the RCL paper, temperature factor = $\exp[-(B_{11}h^2+B_{12}hk\ldots)]$, and therefore the cross terms of RCL have been divided by a factor of two.

Table 5. *Root-mean-square components of thermal displacement along principal axes R_1, R_2 and R_3 of vibration ellipsoids and r.m.s. radial displacements for β-$UO_2(OH)_2$*

	Displacement along			R.m.s. radial
	R_1	R_2	R_3	displacement
U	0·071 (12)	0·102 (7)	0·108 (5)	0·164 (2) Å
O(1)	0·101 (35)	0·142 (32)	0·183 (35)	0·253 (29)
O(2)	0·079 (46)	0·125 (32)	0·175 (29)	0·229 (23)

Table 6. *Orientation of thermal vibration ellipsoids for β-$UO_2(OH)_2$*

		Angle of R with		
	R	a	b	c
U	1	31 (10)°	117 (13)°	76 (11)°
	2	110 (16)	149 (35)	113 (53)
	3	113 (21)	105 (46)	28 (45)
O(1)	1	145 (32)	82 (27)	56 (27)
	2	121 (35)	126 (36)	128 (36)
	3	75 (25)	143 (35)	56 (29)
O(2)	1	133 (21)	118 (22)	56 (33)
	2	109 (29)	118 (30)	145 (34)
	3	130 (18)	42 (22)	100 (23)

Thermal expansion

Experimental

Elevated temperature X-ray powder patterns and five of the six room-temperature patterns were recorded with a Unicam 19 cm high-temperature camera and copper $K\alpha$ radiation. Temperatures were calibrated using silver as a thermal expansion standard. Temperature control to within ± 5 °C was achieved by voltage stabilization. The knife-edge calibration of the 19 cm camera was checked by taking one room-temperature pattern with a Siemens 11·46 cm camera using the Straumanis film-loading technique.

Only lines with θ values greater than 60° were used for the lattice parameter determination. The coarsely crystalline nature of the sample made it easy to identify the α_1 and α_2 components when line overlap occurred. All the reflexions observed for $\theta > 60°$ fulfilled the condition h,k,l all even or all odd; at 21° there are 44 such reflexions in the range $60° < \theta < 85°$ and all except 066 and 171 were positively identified at least once, if not at 21 °C, then at some elevated temperature. In general, about 50 to 60 α_1 and α_2 lines could be measured in any one film; of these about 40 could be unambiguously indexed and were used for lattice parameter calculations. An exception to this occurred at the maximum experimental temperature (317 °C), when only 17 lines could be measured and 14 used for calculations.

Lattice parameters were calculated using a program developed by Walker (1963), based on Hess's (1951) method. Values of θ were also calculated on the basis of the refined lattice parameters and the computed drift constant in order to confirm that all observed reflexions were correctly indexed.

Thermal expansion was also measured optically by heating single crystals to 300 °C in both dry argon and dry air in a Leitz heating stage on a Metallux microscope and taking 35 mm photographs of the {001} surface at various temperatures. Specimen temperatures were measured by a thermocouple, calibrated *in situ* using reliable melting points. The photographs were enlarged and small surface features such as growth steps were used as reference points to determine thermally-induced dimension and shape changes within the {001} plane.

Results

The six X-ray diffraction determinations of each lattice parameter of the orthorhombic unit-cell at 21 °C gave values in the following ranges (Cu $K\alpha_1 = 1{\cdot}54051$, Cu $K\alpha_2 = 1{\cdot}54433$ Å):

$a = 5{\cdot}6432$ to $5{\cdot}6442$ Å
$b = 6{\cdot}2864$ to $6{\cdot}2873$
$c = 9{\cdot}9360$ to $9{\cdot}9374$

There was no significant difference in results either between cameras or between the four different specimens used. The individual values were weighted according to their respective variances and used to calculate the following mean values and standard deviations of the means:

$a = 5{\cdot}6438 \pm 0{\cdot}0001$ Å
$b = 6{\cdot}2867 \pm 0{\cdot}0001$
$c = 9{\cdot}9372 \pm 0{\cdot}0002$.

Thus

$V = 352{\cdot}58 \pm 0{\cdot}02$ Å^3

and

$D_x = 5{\cdot}7274 \pm 0{\cdot}0004$ g.cm^{-3} .

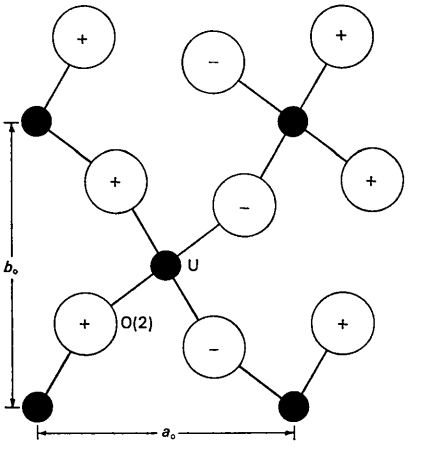

Fig. 3. A projection on {001} of uranium and O(2) atoms in a single layer of β-$UO_2(OH)_2$. (Atom sizes not to scale.)

The low computed standard deviations in a, b and c reflect the fact that experimental values significantly different from the weighted mean values were associated with larger variances than those close to the mean values. The large number of strong high-angle reflexions, including four in the range $80° \leq \theta \leq 84{\cdot}6°$, also contributed to the precision of this work.

The lattice parameters tend to be larger than those of RCL and of Dawson, Wait, Alcock & Chilton (1956), and are more precise.

The thermally-induced changes in a, b, c and V, relative to their values at 21 °C, are plotted against temperature in Fig. 1. The thermal expansion in b and contraction in a are larger than the changes in c and V, and they tend to saturation at about 260 °C. From 260 to 317 °C all three lattice parameters increase by similar, small amounts. The computed standard deviations in the lattice parameters at temperatures above ambient vary from 0·0001 to 0·0005 Å in a, 0·0002 to 0·0006 Å in b, and 0·0004 to 0·0007 Å in c, with the exception of the results at 317 °C where the standard deviations are 0·0014, 0·0030 and 0·0025 Å respectively. However the scatter in Fig. 1 is larger than can be explained by these possible errors and the observed fluctuations in temperature. Three different specimens were used to obtain the results in Fig. 1. It is believed that the scatter is due to a variation from specimen to specimen in the difference between specimen temperature and thermocouple temperature (which from the silver calibration reached 160 °C at a specimen temperature of 300 °C).

The extreme anisotropy in thermal expansion of β-$UO_2(OH)_2$ would indicate that there would be thermally-induced shape changes in single crystals of this material, as was indeed observed by hot-stage microscopy. The largest changes occur in the {001} plane, in which the thermal contraction in a and expansion in b cause the angle between the [110] and [$\bar{1}$10] edges of a crystal to decrease from its room-temperature value of 83° 50′ with increase in temperature. The change in angle may be calculated from the values of a and b, and in Fig. 2 the calculated decreases in angle at various temperatures are compared with the values determined by optical microscopy. There is good agreement between the X-ray diffraction and optical results. The thermal distortion reaches a constant limiting value of 130 ± 2 min above 260 °C. Optical measurements not shown in Fig. 2 suggest that this distortion persists up to at least 380 °C, at which point there are obvious signs of dehydration.

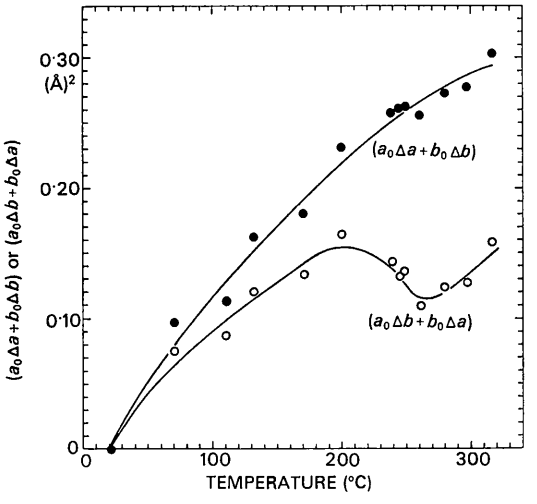

Fig. 4. Changes with temperature in the functions $(a^2 + b^2)$ and (ab) for β-$UO_2(OH)_2$.

Discussion

Fig. 2 demonstrates that the thermally-included shape changes observed in single crystals of β-$UO_2(OH)_2$ can be fully explained by anisotropic thermal expansion of the crystal lattice. The following factors indicate that this is not caused by changes of material composition but is a true thermal expansion effect:

(1) the X-ray 'powder' samples were sealed within silica capillaries, to limit decomposition;
(2) specimens used for exposures at 244 and 248 °C reverted to their original lattice parameters on cooling to 21 °C;
(3) shape changes observed in the hot-stage microscope, in which composition changes in a crystal were not hindered, depended only on temperature and not on whether the observations were made during heating or cooling. Heating and cooling rates were about 5 °C. minute^{-1}.

Three features aid interpretation of the anisotropic thermal expansion of β-$UO_2(OH)_2$. The first is the fact that the major thermally-induced changes occur within the {001} plane, and thus within the layers which make up the structure of this material. Each layer is composed of octahedra consisting of a central uranium atom surrounded by six oxygen atoms. Four of these oxygen atoms are hydroxyl oxygen atoms [O(2)], and each is shared by two octahedra so that the a and b spacings are determined solely by the lengths and directions of the U–O(2) bonds. Thus the large thermally-induced changes in a and b can only be caused by changes in the lengths and/or directions of the U–O(2) bonds. The arrangement of U and O(2) atoms within one layer is shown in Fig. 3, in which the O(2) atoms indicated + are located 0·82 Å above the plane of the U atoms, and those shown − are 0·82 Å below the plane. The other two oxygen atoms in each octahedron are not shown in Fig. 3. They are uranyl oxygen atoms [O(1)] and are not shared with any other octahedron but are probably hydrogen-bonded to O(2) atoms in octahedra of the neighbouring layers. Thus the c spacing, in which thermally-induced changes are small and apparently complex, is determined by the lengths and directions of the more complicated series of bonds U–O(2), O(2)–H·····O(1) and O(1)–U.

The second aid to interpretation of the expansion behaviour is the discovery that, although the lattice contracts along [100] and expands strongly along [010], with both effects reaching saturation at about 260 °C, thermal expansion along [110] shows no discontinuity or change in direction from 21 to 317 °C. This was first suggested by hot-stage microscopy, but may be clearly demonstrated using the more accurate X-ray results. It implies that (a^2+b^2), or alternatively $(a_0\Delta a+b_0\Delta b)$, should be a smooth function of temperature from 21 to 317 °C. Here a and b are the lattice parameters at elevated temperature, a_0 and b_0 are the room-temperature values, and Δa and Δb are the changes relative to a_0 and b_0. The smooth variation of $(a_0\Delta a+b_0\Delta b)$ with temperature is shown in Fig. 4 which, to illustrate the effects of the shape-change saturation at 260 °C, also contains a plot of $(a_0\Delta b+b_0\Delta a)$, the change in area ab.

The significance of the smooth thermal expansion along [110] may be appreciated by referring to Fig. 3. The spacing between U atoms along ⟨110⟩ is defined by a series of U–O(2) bonds, each slightly inclined to ⟨110⟩, and the smooth and continuous thermal expansion along [110] suggests smooth and continuous thermally-induced changes in bond length and inclination to ⟨110⟩. However the large changes in a and b, which reach saturation at about 260 °C, have already been attributed to changes in the lengths and/or directions of the U–O(2) bonds, and any such change would have to reach a limit at about 260 °C. The only compromise which satisfies both requirements is expansion of the U–O(2) bonds with temperature in a normal manner, with their inclination to ⟨110⟩ either not changing or varying smoothly with temperature, but with their directions within the crystal lattice changing from 21 to 260 °C and thereafter remaining constant. This variation in direction could only be achieved by rotation of each U–O(2) bond about ⟨110⟩.

The final aid to the interpretation is the fact that the distortion in the structure reaches a well-defined limit (at about 260 °C – see Figs. 1 and 2). The existence of a limit must be an integral part of any explanation for the anisotropic thermal expansion, and the magnitude of the limiting distortion (Fig. 2) affords a quantitative check. This point will be used in the subsequent argument.

In the discussion which follows, the inclination of each U–O(2) bond to ⟨110⟩ is assumed to remain constant, so that in the absence of rotation of the U–O(2) bonds about ⟨110⟩ a regular increase in bond length would cause an isotropic expansion within the {001} plane. The anisotropic thermal expansion is attributed to the additional effect of rotation of the U–O(2) bonds about ⟨110⟩. Unless otherwise stated the isotropic thermal expansion of the entire layer is ignored, and the bond rotation is treated as though unaccompanied by changes in either bond length or inclination to ⟨110⟩.

A possible reason for a thermally-induced rotation of the U–O(2) bonds about ⟨110⟩ may be deduced from the O(2) thermal vibration parameters and consideration of the crystal structure. Of the three principal axes of the vibration ellipsoid for O(2), R_1 and R_2 are virtually coplanar with O(2) and its two bonded U atoms whereas R_3 appears to be normal to this plane [actual angle $73\pm21°$ (standard deviation)]. The dominance of R_3 over R_1 and R_2 then suggests that vibration of O(2) normal to the plane of its bonds is easier than vibration within the plane, so that superimposed on an approximately isotropic vibration of O(2) about its mean position there is a libration of O(2) about its two bonded U atoms, *i.e.* about ⟨110⟩.

The likely effect of libration of the O(2) atom about ⟨110⟩ may be demonstrated by referring to Fig. 5, which is a projection on {100} of all the U, O(1) and O(2) atoms within the volume enclosed by a_0, $2b_0$ and c_0. A feature of the structure is the array of continuous channels, parallel to ⟨100⟩ and spaced at intervals of $b_0/2$ and $c_0/2$. Libration of each O(2) atom about the line joining its two bonded U atoms would tend to move the O(2) atom into and out of one of these channels. It seems reasonable to expect that with increasing temperature there would be a net displacement into the channel; in other words, a net rotation of the U–O(2)–U plane about the U–U direction. There is a natural limit to the rotation and, thus, a limit to the distortion of the structure, when the O(2) attains its maximum intrusion into the channel. This occurs when the O(2) atoms achieve their maximum displacement normal to the {001} plane containing their bonded U atoms. At this point the projections of the O(2) atoms on {001} fall exactly on the [110] and [1$\bar{1}$0] directions joining adjacent U atoms.

If the O(2) atoms in Fig. 3 are moved in this way, the projected edges of the planar O(2) configuration around each U atom become more nearly parallel to the [100] and [010] directions. In addition the tilt of the plane to {001} increases. Since thermal expansion of the plane is being ignored, and since the b parameter

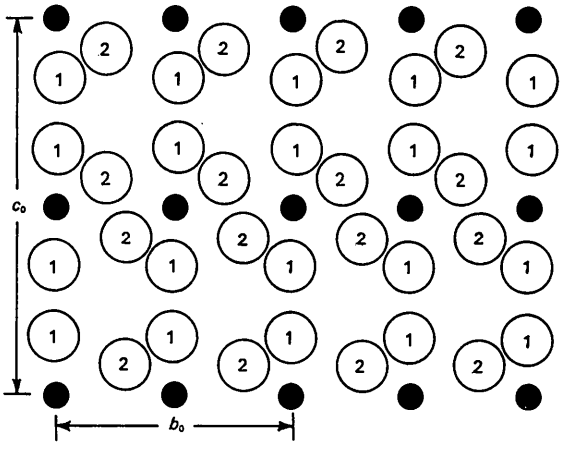

Fig. 5. A projection on {100} of U, O(1) and O(2) atoms of β-$UO_2(OH)_2$ in a volume bounded by a_0, $2b_0$ and c_0. (Atom sizes not to scale.)

is equal to twice the spacing between O(2) atoms in the [010] direction, improved alignment of O(2) along [010] must cause an increase in b. And since thermal expansion along $\langle 110 \rangle$ is being ignored, there must be a corresponding decrease in a. The effect of a general isotropic expansion in bond length would be to lessen the decrease in a and increase the expansion in b. However the distortion of the structure would not be affected and this allows the model to be tested for quantitative agreement with experiment. The predicted maximum decrease in the angle between the [110] and $[\bar{1}10]$ directions is 146 ± 65 min (standard deviation), in satisfactory agreement with the result of 130 ± 2 min found by X-ray diffraction. The large standard deviation for the predicted angle change is mainly due to the uncertainties in the O(2) position parameters. However, the anisotropic thermal expansion in a and b appears to be adequately explained in terms of a net rotation of the U–O(2) bonds about $\langle 110 \rangle$.

The discussion has so far concentrated on changes within the {001} layers. Without a detailed knowledge of thermally-induced changes in the U–O(1) and O(2)–H·····O(1) bond lengths and directions it is impossible to discuss changes in the c parameter in other than a general way. Figs. 1 and 4 indicate that changes in c follow the same pattern as changes in the area ab; in the latter case the overall effect is the result of simultaneous expansion and distortion and it is logical to attribute the cyclic variation in c to a similar combination of events.

The following positional parameters for the O(1) and O(2) atoms in the fully-distorted structure have been calculated on the assumption that rotation of the U–O(2) bonds causes a rotation of each octahedron of oxygen atoms, without any change in shape of the octahedron. This assumption is partly justified on the basis that the only bonds affected by the rotation are the relatively weak O(2)–H·····O(1) bonds. The parameters for O(2) should be substantially correct, but discrepancies in the O(1) parameters are likely as a result of independent vibrations and librations of the O(1) atom.

$$\begin{aligned} \text{O(1):}\ & x = 0{\cdot}180 \\ & y = 0{\cdot}490 \\ & z = 0{\cdot}500 - 1{\cdot}511/c \\ \text{O(2):}\ & x = 0{\cdot}247 \\ & y = 0{\cdot}247 \\ & z = 0{\cdot}905/c \end{aligned}$$

The values of z involve the lattice dimension c since this explanation for the anisotropic thermal expansion cannot predict likely changes in the interlayer distance. It appears that the interlayer distance decreases with distortion, since the layer thickness from O(1) to O(2) increases more than the c parameter. Also, if the positional parameters given above are correct, the O(1)–O(2) interlayer contact distances change with distortion from the values in Table 4 to ones which are virtually equal to each other and intermediate between the Table 4 distances. This would suggest that bifurcated hydrogen bonds exist in the fully-distorted structure.

Conclusions

β-$UO_2(OH)_2$ may be added to the growing list of materials which not only have anisotropic thermal expansion coefficients, but which exhibit a thermal contraction in at least one of the unit-cell parameters. This thermal distortion of the lattice reaches a well-defined limiting value, beyond which the thermal expansion coefficients are all positive and approximately isotropic.

Improved values of positional and vibrational parameters for the uranium and oxygen atoms in the structure permit an explanation of the thermal distortion in terms of a net rotation of the oxygen octahedron surrounding each uranium atom. However, it would be desirable to confirm this interpretation by a structure determination at elevated temperature.

The authors are indebted to Mr B. W. Edenborough of the Chemical Engineering School, University of New South Wales, for supplying the mixture of α- and β-$UO_2(OH)_2$. Messrs J. G. Napier, W. J. Buykx and K. G. Watson assisted in the operation of the high-temperature X-ray camera.

References

Busing, W. R., Martin, K. O. & Levy, H. A. (1962*a*). *ORFLS*. ORNL-TM-305, Oak Ridge National Laboratory, Tennessee.

Busing, W. R., Martin, K. O. & Levy, H. A. (1962*b*). *ORFFE*. ORNL-TM-306, Oak Ridge National Laboratory, Tennessee.

Cromer, D. T. (1965). *Acta Cryst.* **18**, 17.

Dawson, J. K., Wait, E., Alcock, K. & Chilton, D. R. (1956). *J. Chem. Soc.* p. 3531.

Harris, L. A. & Taylor, A. J. (1962). *J. Amer. Ceram. Soc.* **45**, 25.

Hess, J. B. (1951). *Acta Cryst.* **4**, 209.

International Tables for X-ray Crystallography (1962). Vol. III, p. 202, 212. Birmingham: Kynoch Press.

Roof, R. B. Jr, Cromer, D. T. & Larson, A. C. (1964). *Acta Cryst.* **17**, 701.

Walker, D. G. (1963). Australian Atomic Energy Commission Report AAEC/TM189.